Time-Dependent Nonlinear Hadley Circulation

MING FANG AND KA KIT TUNG

Department of Applied Mathematics, University of Washington, Seattle, Washington

(Manuscript received 23 May 1997, in final form 10 July 1998)

ABSTRACT

The time-dependent Hadley circulation is studied numerically in a nonlinear, nearly inviscid, axially symmetric primitive equation model, with the heating varying periodically on an annual cycle. The annual average of the Hadley circulation strength in this model with time-dependent heating is about a factor of 2 stronger than the steady-state response to the annual mean heating and is closer to the observed strength in the real atmosphere. This is caused by the fact that heating centered off-equator tends to produce stronger meridional circulation in the winter hemisphere than in the case when the heating maximum is located at the equator, as pointed out previously by Lindzen and Hou. However, unlike the steady-state solutions, there is no abrupt change as the heating center is moved off the equator.

The temperature response in this time-dependent model is simple to understand. In the tropical region, where there is a variable, but persistent, Hadley circulation, the temperature is homogenized latitudinally. In the high-latitude region, where there is no meridional circulation (in the absence of the eddies), the temperature response goes through an annual cycle with a phase lag relative to the phase of the heating. This response is as predicted by the simple time-dependent temperature equation in the absence of meridional circulation.

1. Introduction

Although the zonal mean circulation in the extratropics is believed to be driven by eddies (departures from the zonal mean), the zonal mean circulation in the tropical region can exist even without them. Theoretical studies of axisymmetric models aim to understand this simpler subset of the possible circulation systems. An excellent review can be found in Lindzen (1990, chap. 7).

With the notable exceptions of Hack et al. (1989), Hack and Schubert (1990), and Liu and Mak (1995), past theoretical studies of the Hadley circulation have focused on understanding the steady states achieved by axisymmetric models (Schneider and Lindzen 1977; Schneider 1977; Held and Hou 1980; Lindzen and Hou 1988; Hou and Lindzen 1992; Plumb and Hou 1992; Fang and Tung 1996, 1997). We note, however, that the adjustment time for an axially symmetric model to obtain a steady state is of the order of 100 days or even longer, which is longer than the seasonal timescale. Since heating varies on a seasonal timescale in the atmosphere, it is of interest to study the time-dependent solution corresponding to an annually periodic thermal forcing, and to compare it with the steady solution.

In this paper, we use a time-dependent axisymmetric primitive equation model to investigate the temporal variability of the Hadley circulation systematically. The model, boundary conditions, and the parameters used in this paper are described in section 2. The steady solutions are reviewed briefly in section 3. The time-dependent solutions are presented and discussed in section 4 and the concluding remarks follow in section 5.

2. The model

a. The primitive equations

In this simple model, we consider a set of steady, axially symmetric primitive equations for a Boussinesq fluid on a sphere of radius a rotating with rate Ω, confined between the bottom solid surface and a stress-free lid at height H. Let Θ be the (potential) temperature, Θ_0 the constant reference temperature (globally averaged surface temperature), Q the diabatic heating rate per unit mass, and (u, v, w) the velocity of the fluid in the longitudinal, latitudinal (ϕ), and the vertical (z) direction, respectively. The equations are

Corresponding author address: Dr. Ka Kit Tung, Department of Applied Mathematics, University of Washington, Box 352420, 412 Guggenheim Hall, Seattle, WA 98195.
E-mail: tung@amath.washington.edu

$$\frac{\partial u}{\partial t} + \frac{v}{a}\frac{\partial u}{\partial \phi} + w\frac{\partial u}{\partial z} - \frac{uv}{a}\tan\phi - 2\Omega v \sin\phi = \nu\nabla^2 u \quad (1)$$

$$\frac{\partial v}{\partial t} + \frac{v}{a}\frac{\partial v}{\partial \phi} + w\frac{\partial v}{\partial z} + \frac{u^2}{a}\tan\phi + 2\Omega u \sin\phi = \nu\nabla^2 v - \frac{1}{a}\frac{\partial \Phi}{\partial \phi} \quad (2)$$

$$\frac{1}{a}\frac{\partial(v\cos\phi)}{\cos\phi\partial\phi} + \frac{\partial w}{\partial z} = 0 \quad (3)$$

$$\frac{\partial \Phi}{\partial z} = g\frac{\Theta}{\Theta_0} \quad (4)$$

$$\frac{\partial \Theta}{\partial t} + \frac{v}{a}\frac{\partial \Theta}{\partial \phi} + w\frac{\partial \Theta}{\partial z} = \kappa\nabla^2\Theta + \frac{Q}{C_p}, \quad (5)$$

$$Q/C_p = \frac{\Theta_E - \Theta}{\tau}, \quad (6)$$

where ν is the kinematic viscosity coefficient and κ is the coefficient of thermal diffusivity; C_p is the specific heat of the gas at constant pressure. The diabatic heating is here parameterized by the Newtonian cooling law in (6), as in Schneider (1977), Held and Hou (1980), and Lindzen and Hou (1988). This is done so that comparison with these prior results can be made with respect to the effects of time dependence. It should be noted, however, that the use of Newtonian cooling gives rise to a broader positive heating region than is the case in the real atmosphere, where heating is concentrated in narrow regions. The readers are referred to Fang and Tung (1996), where the intertropical convergence zone (ITCZ) is incorporated in a simple model. Also, the theormal relaxation time τ is generally a function of space (see Fang and Tung 1996, 1997). In this paper, we consider only constant τ.

Following Lindzen and Hou (1988), the equilibrium potential temperature used in our numerical calculations here are given in the analytic form:

$$\Theta_E = \Theta_0 - \Delta_H(\mu - \mu_0)^2 + \Delta_V z, \quad (7)$$

where $\mu \equiv \sin\varphi$. Unlike that used in Lindzen and Hou (1988), where the location of the maximum surface temperature μ_0 is a fixed constant, here it varies in time according to

$$\mu_0(t) = \mu_{0\,\max}\sin\left(\frac{2\pi t}{360\text{ days}}\right). \quad (8)$$

b. Boundary conditions

The boundary conditions for the velocities are no-slip conditions at the bottom and stress-free lid at the top. The boundary is considered to be insulated so that no heat flux crosses it. There is no poleward velocity—that is, $v\cos\phi = 0$—at the poles.

c. Nondimensionalization

As in Fang and Tung (1994), nondimensional variables are introduced by asterisks as follows: $z^* = z/H$; $t^* = 2\Omega t$; $\tau^* = 2\Omega\tau$; $(u^*, v^*) = (u, v)/U$; $w^* = (w/U)(a/H)$; $\Phi^* = \Phi/2\Omega aU$; $\nabla^{*2} = H^2\nabla^2$; and

$$\Theta^* = \frac{\Theta}{\Theta_0}\frac{gH}{2\Omega aU} = \frac{R_H}{\text{Ro}}\frac{\Theta}{\Theta_0}.$$

Here U is a typical zonal velocity, $\text{Ro} \equiv U/(2\Omega a)$ is Rossby number, and $R_H \equiv gH/(2\Omega a)^2$. After the nondimensionalization process, the superscript asterisks for the nondimensional variables are dropped without confusion:

$$\frac{\partial u}{\partial t} + \text{Ro}\left(v\frac{\partial u}{\partial \phi} + w\frac{\partial u}{\partial z} - uv\tan\phi\right) - \sin\phi v = E\frac{\partial^2 u}{\partial z^2} \quad (9)$$

$$\frac{\partial v}{\partial t} + \text{Ro}\left(v\frac{\partial v}{\partial \phi} + w\frac{\partial v}{\partial z} + u^2\tan\phi\right) + \sin\phi u = E\frac{\partial^2 v}{\partial z^2} - \frac{\partial \Phi}{\partial \phi} \quad (10)$$

$$\frac{1}{\cos\phi}\frac{\partial(v\cos\phi)}{\partial\phi} + \frac{\partial w}{\partial z} = 0 \quad (11)$$

$$\frac{\partial \Phi}{\partial z} = \Theta \quad (12)$$

$$\frac{\partial \Theta}{\partial t} + \text{Ro}\left(v\frac{\partial \Theta}{\partial \phi} + w\frac{\partial \Theta}{\partial z}\right) = \frac{E}{\text{Pr}}\frac{\partial^2\Theta}{\partial z^2} + \frac{\Theta_E - \Theta}{\tau}. \quad (13)$$

The values of the parameters used are $\Delta_H = \frac{1}{6}°$, $\Gamma = 6°\text{ km}^{-1}$, $\Gamma_d = 9.8°\text{ km}^{-1}$, $H = 15$ km, $\Theta_0 = 300$ K, $\nu = 3.5\text{ m}^2\text{ s}^{-1}$, and $\tau = 20$ days. These lead to $\Delta_V \equiv \Gamma_d - \Gamma = 3.8°\text{ km}^{-1}$ and $E = 1 \times 10^{-4}$. The typical velocity U is taken from the thermal equilibrium solution as $gH\Delta_H/(2\Omega a)$ and it leads to a thermal Rossby number of $\text{Ro} = R = gH\Delta_H/(2\Omega a)^2 = 0.0283$. The Prandl number $\text{Pr} \equiv \nu/\tau$ is takein to be 1.

d. The ''nearly inviscid'' limit

The rationale for studying the so-called nearly inviscid limit was discussed by Held and Hou (1980). This is the limit of E small but nonzero, that is, $E \to 0^+$. For moderate to large values of E, it is known that the meridional circulation in the solution is viscosity driven and sensitive to the value of E chosen (see Fang and Tung 1994). However, as E becomes smaller, the tropical circulation becomes nonlinearity dominated, and the de-

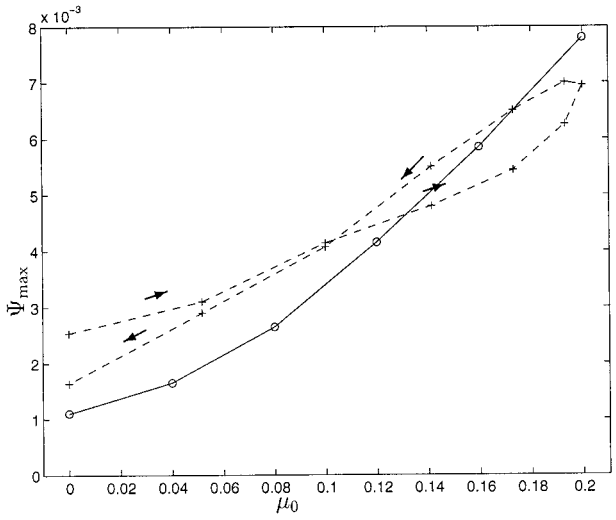

FIG. 1. The dimensionless strength of the winter cell for various μ_0. For the steady solution (solid line), the strength is defined as the global maximum of the absolute value of the streamfunction. For the time-dependent solution (dashed line), plotted is the strength of the counterclockwise cell in the Southern Hemisphere.

pendence on the exact value of E becomes negligible. It is this nearly inviscid limit that we wish to study here as well. Numerical instabilities prevent numerical calculations of steady-state solutions for values of E much less than the value we used ($E = 10^{-4}$). At this value of E, symmetric instabilities are not suppressed, and they show up as ''noise'' in some of the plots.

3. The steady solution

For each fixed location μ_0 of the heating maximum, the model circulation can reach a steady state. The solution is obtained and discussed by Held and Hou (1980) for $\mu_0 = 0$, and by Lindzen and Hou (1988) for $\mu_0 \neq 0$. We solve the problem numerically again and present the results briefly here for the purpose of comparison to its time-dependent counterpart.

In the steady solution, the pattern and the strength of the meridional circulation strongly depend on μ_0. The location and the maximum value of the zonal jet depend on μ_0 as well.

When the heating center is placed off the equator, the strength and size of the winter cell are enhanced, while the strength and size of the summer cell decrease and become almost negligible. This acute sensitivity to μ_0 being slightly off the equator was first noted by Lindzen and Hou (1988). Figure 1 shows (in solid line) the dependence of the strength of the circulation on the heating center. Shown is the maximum strength of the ''winter'' circulation as a function of μ_0. The winter hemisphere is defined here as the hemisphere opposite to $\mu_0(t)$. For positive values of μ_0, this winter circulation occurs in the Southern Hemisphere. It is noted that the increase in the strength is monotonic with respect to μ_0, with a steep slope. The strength of the circulation for $\mu_0 = 0.06$ (about 3.5°) is about twice that for $\mu_0 = 0$. The strength for $\mu_0 = 0.16$ (9°) is more than five times. We will note that this sensitive dependency on μ_0 is a feature of the steady-state solution only.

For the purpose of later comparison with time-dependent solution where μ_0 goes through an annual cycle, we perform calculations where μ_0 takes on each of the values in the annual cycle as specified in (8), but where the solution is allowed to reach the steady state for each chosen value of μ_0. The steady solution is then ''annually averaged'' in the following way:

$$\overline{X}_s = \frac{1}{N}\sum_{i=1}^{N} X_s[\mu_0(t_i)], \tag{14}$$

where t_i is equally spaced time in an annual cycle, $\mu_0(t_i)$ is the location of the heating center at time t_i according to (8), N is total number of partitions of an annual cycle, and X_s is the steady state of X corresponding to $\mu_0(t_i)$. The ''annual mean'' meridional circulation calculated this way is symmetric about the equator and has about the same extent as the steady solution corresponding to $\mu_0 = 0$. *Remarkably, the strength of the annual mean circulation is twice as strong as that in the case of* $\mu_0 = 0$.

The horizontal gradient of the temperature is flat in the inviscid core of the circulation region. More precisely, the temperature is flat within the strong circulation cell in the winter hemisphere. [The temperature is not flat within the much weaker ''summer'' circulation cell because absolute angular momentum is less conserved there (see Fang and Tung 1996). This nonabsolute-angular-momentum-conserving behavior may be due to the fact that the circulation is weak in this region and so viscous effects become relatively more significant there.] The temperature distribution for $\mu_0 = 0.2$ is shown in Fig. 2a, where the solid lines are for the steady-state temperature and the dashed lines are for the radiative equilibrium temperature. The annual mean of the steady solutions is shown in Figure 2b, where the solid line is for the mean temperature and the dashed line is for the temperature corresponding to the steady solution for $\mu_0 = 0$. It is noted that the annual mean temperature in the Tropics is lower than the steady temperature corresponding to $\mu_0 = 0$, implying a stronger upwelling, leading to a smaller equator–pole temperature contrast. The vertically averaged temperatures for various μ_0 have been calculated and it is found that it is not in geostrophic balance with the zonal wind at the top. The geopotential at the surface in the circulation region is nonzero and plays an important role in maintaining the geostrophic balance between the geopotential gradient and the zonal wind at the top [see the discussion in Fang and Tung (1996)].

The zonal wind is given by the radiative-equilibrium solution in the high latitudes where there is no meridional circulation. Inside the circulation region in the

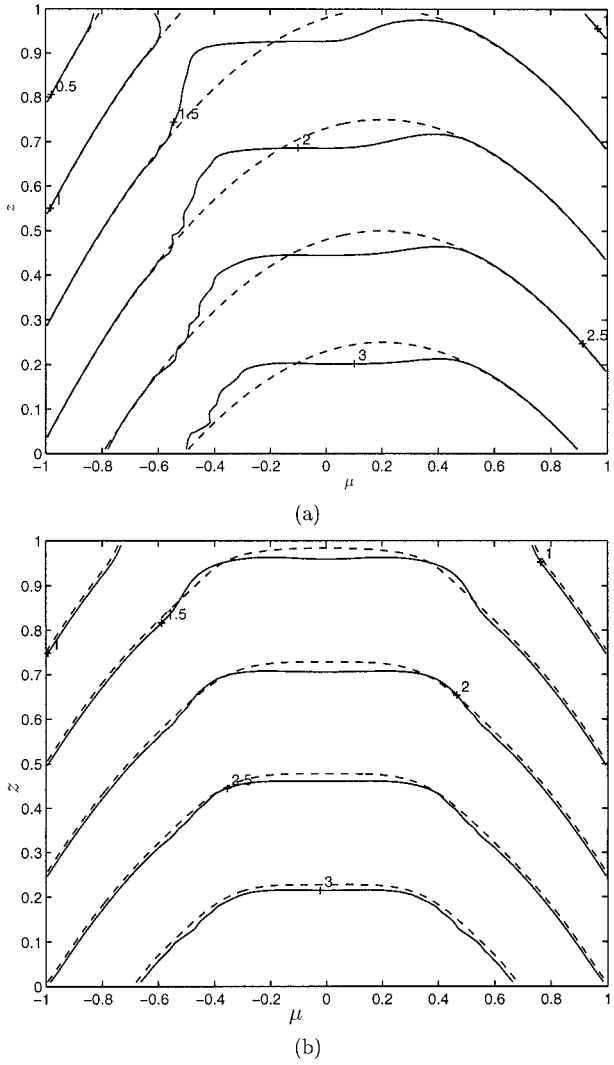

FIG. 2. (a) Temperature distribution for $\mu_0 = 0.2$, where the solid lines show the temperature and the dashed lines show the equilibrium temperature. (b) Annual mean of the steady temperature (solid lines), and the steady temperature corresponding to $\mu_0 = 0$ (dashed lines). The temperature contours shown are $(\Theta - 125\ \text{K})/50\ \text{K}$.

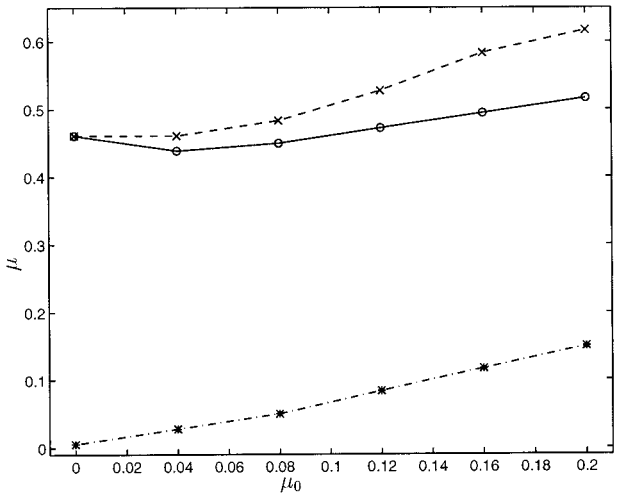

FIG. 3. The position of the easterly maximum (dash–dotted line with "*"), of the winter jet (solid line with "○"), and of the summer jet (dashed line with "×"). For compactness of the figure, the winter jet's position is reflected about the equator and plotted in the same hemisphere as the summer jet.

Tropics it is close to an absolute-angular-momentum-conserving solution. Since the summer cell is almost negligible when μ_0 is large, the value of the summer jet is approximately given by the radiative equilibrium solution, which is much weaker than the absolute-angular-momentum-conserving solution, at the jet position. The latitude where the conserved absolute-angular momentum originates [defined in Lindzen and Hou (1988) as ϕ_1] moves off the equator to the poleward side of the heating center and causes a strong winter jet. The maximum of the zonal wind in the winter hemisphere is a monotonically increasing function of μ_0, while the maximum of the zonal wind in the summer hemisphere is a monotonically decreasing function. The maximum of the easterly zonal wind is also a monotonically increasing function of μ_0. The positions of the zonal jets are shown in Fig. 3. The solid line is for the winter jet and the dashed line is for the summer jet. As in Lindzen and Hou (1988), we found that the winter jet is centered closer to the equator than the summer jet, which is the case in the real atmosphere. The position of the winter jet is also a good indication of the edge of the winter circulation cell and we found that it is not sensitive to the displacement of the heating center. [The jet maximum is always located around 30°, which is not as given by the simple model solution of Held and Hou (1980), as pointed out by Lindzen and Hou (1988)]. Figure 3 also shows the locations of the maximum easterlies in a dash–dotted line. It is almost linearly proportional to the displacement of the heating center off the equator. The annual mean of the steady zonal wind distribution is also calculated according to (14). It is noted that the tropical easterlies in the mean field are much stronger than those in the equatorially symmetric case and the easterly region is also wider. In the mean field, the jet position is almost the same as that in the equatorially symmetric case while the meridional gradient becomes stronger on the poleward side of the jet.

4. Time-dependent solution

a. Circulation

The numerical calculations for the time-dependent case are performed with $\mu_{0\,\max} = 0.2$. The initial condition is the steady-state solution corresponding to $\mu_0 = 0$. A periodic solution establishes itself in about 4 months. As in the steady solution, the meridional plane can be divided into two regions: a tropical region where

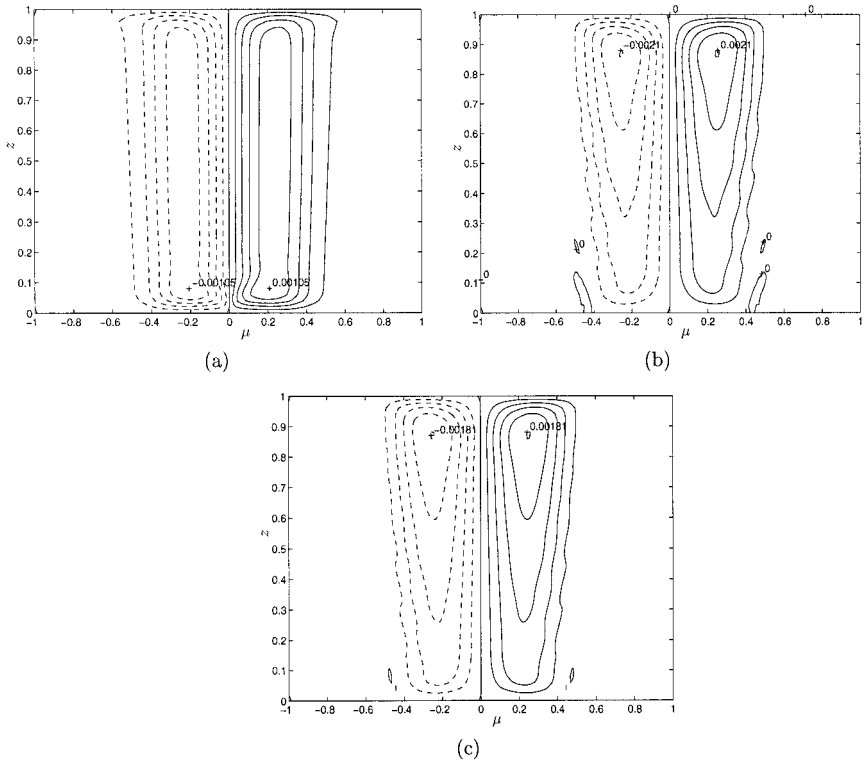

FIG. 4. The dimensionless streamfunction for (a) the steady-state solution corresponding to $\mu_0 = 0$, (b) the annual average of the steady-state solutions according to (14), and (c) the annual average of the time-dependent solution corresponding to annually periodic heating.

a strong heating-induced meridional circulation exists, and a subtropical-to-polar region where the meridional circulation is mainly driven by the small viscosity and is almost negligible.

Figure 4 shows the equatorially symmetric meridional circulation from (a) the *steady* solution corresponding to *steady* symmetric heating; (b) the annual average, according to (14) of the *steady*-state solution for various steady displacements of the heating maximum; and (c) the true annual average of the time-dependent solution in the presence of an annually varying heating. All three circulations are remarkably similar, except the last two (b and c) are about a factor of 2 stronger than a.

In cases b and c, although the annually *averaged* circulation is symmetric about the equator, the actual circulation is never symmetric and is instead dominated by a single cell during most of the year. The circulation in this cell is strongly nonlinear—it is nearly angular-momentum conserving—and therefore it is expected that the average of the solutions corresponding to different heating is not necessarily the same as the solution corresponding to the averaged heating. This explains why b and c are different from a. The circulations that enter into the averages in b and c are mostly asymmetric about the equator. These single, summer-to-winter cells are much stronger than the symmetric two cells studied by Held and Hou (1980). Lindzen and Hou (1988) gave a detailed analysis based on the ''equal area'' rule in potential temperature conservation, and the principle of angular momentum conservation.

As mentioned before, the time-dependent model meridional circulation is dominated by a single cell during most of the year. In Fig. 1, the strength of that circulation in the time-dependent solution is plotted (in dashed line) as a function of $\mu_0(t)$, along with the strength of the steady-state circulation (in solid line) corresponding to the same, but fixed, values of μ_0. Since only positive values of μ_0 are shown, plotted here is the strength of the winter circulation—the counterclockwise cell in the Southern Hemisphere. The time-dependent solution generally follows the trend of the steady-state solution in that the strength of the circulation increases monotonically with increasing displacement of the heating maximum away from the equator. While the steady-state circulation at the extreme displacement ($\mu_0 = 0.2$) reaches a magnitude that is eight times that of the case when $\mu_0 = 0$, the time-dependent solution achieves a factor of 7 when $\mu_0(t)$ reaches the same extreme position. One could attribute this to the fact that the time-dependent circulation has not ''attained its full potential'' in the extreme μ_0 position before $\mu_0(t)$ starts to move back toward the equator, when the circulation weakens. Nevertheless, due to inertia, the time-dependent solution does not weaken as much as in the steady

solution for the same μ_0. At $\mu_0(t) = 0$, the circulation strength is about 1.7–2.5 times that of the steady-state solution corresponding to symmetric heating ($\mu_0 = 0$). And the solution is not equatorially symmemtric at the instant when $\mu_0(t)$ crosses the equator (we will come back to this point later).

Figure 1 shows that while the annual averages of the time-dependent and steady circulations are about the same, the time-dependent solution does not have an abrupt change of circulation strength as the heating maximum, $\mu_0(t)$, is moved off the equator. The circulation is never equatorially symmetric in the time-dependent case. Therefore, the steady symmetric circulation's low strength is irrelevant because this (symmetric) state is never realized in the time-dependent solution.

Another difference between the time-dependent solution and the steady-state solution is that the former depends not solely on the location of the heating center μ_0, but also on the direction of the movement of $\mu_0(t)$ in its annual march. Thus, the solution at spring equinox is different from that at autumn equinox. While this behavior is to be expected in a time-dependent solution when there is a ''time lag'' or ''inertia,'' the actual behavior is *opposite* from what one may expect based on simple inertia arguments. Figure 1 shows that the circulation strength decays *faster* as $\mu_0(t)$ moves back toward the equator from its extreme winter solstice position than its earlier increase when $\mu_0(t)$ moves away from the equator toward its extreme position. For example, when $\mu_0(t)$ first moves off the equator toward the Northern Hemisphere, the (nondimensional) circulation strength is 2.5×10^{-3}. This is to be compared to the strength of 1.7×10^{-3} when $\mu_0(t)$ next returns to the equator. (For comparison, the steady circulation strength for $\mu_0 = 0$ is 1.0×10^{-3}. We will use this as a standard unit when comparing circulation strengths.) The situation is obviously more complicated than the picture of single-cell strength conveyed by Fig. 1.

Figure 5 gives a more detailed description of the evolution of the circulations through an annual cycle. In both Figs. 5a and 5b, the solid line indicated the position of $\mu_0(t)$ in its annual march. Although we have said that the circulation is *dominated* by a single winter cell, the single cell picture is strictly true only for 3 months during the northern winter (days 210–300) and 3 months during the southern winter (days 30–120). During the southern winter, $\mu_0(t)$ is in the Northern Hemisphere, and the summer cell in the Northern Hemisphere is almost nonexistent. The winter cell in the Southern Hemisphere strengthens to a value that is seven times that of the steady symmetric solution, before it weakens after solstice as $\mu_0(t)$ moves back toward the equator. As $\mu_0(t)$ crosses the equator, the circulation strength is 1.7 times that of the steady symmetric solution. This is as depicted in Fig. 1.

As $\mu_0(t)$ crosses the equator into the Southern Hemisphere, the counterclockwise circulation in the same (southern) hemisphere becomes the summer cell. The

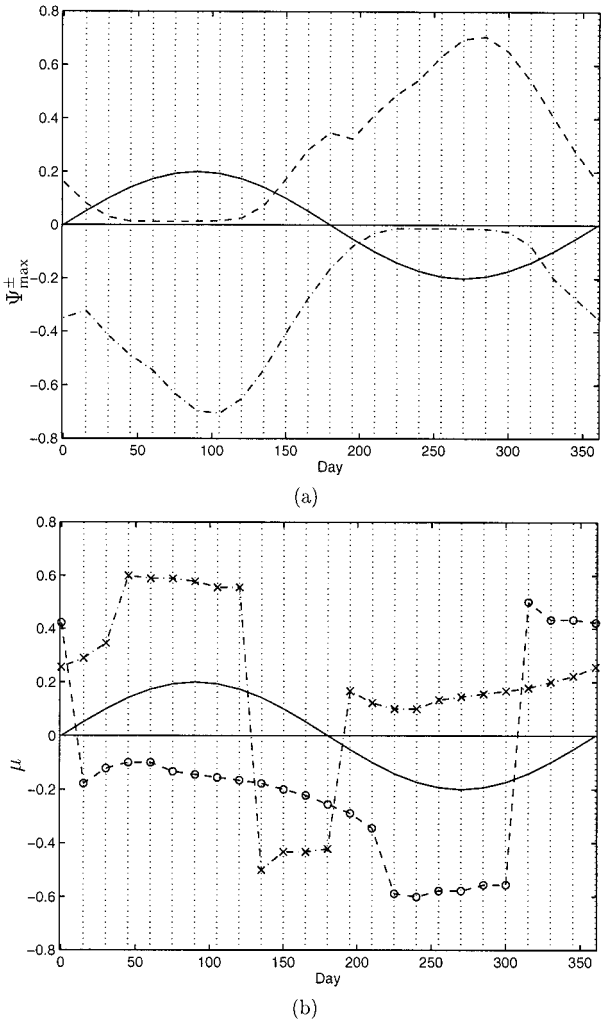

FIG. 5. (a) The maximum (dashed line), i.e., maximum clockwise strength; and the minimum (dash–dotted line), i.e., maximum counterclockwise strength, of the streamfunction and (b) their positions (dash–dotted line with ''×'' for the maximum and dashed line with ''○'' for the minimum) as functions of the time together with $\mu_0(t)$ (solid line). The values of the streamfunction shown have been multiplied by 100.

summer cell decays to almost zero strength and moves to higher latitudes. It stays at zero strength for the full 3 months of summer. The clockwise circulation in the Northern Hemisphere is now called the winter cell. It is not a continuation of the counterclockwise cell in the Southern Hemisphere. In other words, the circulation cell in the Southern Hemisphere does not move to the Northern Hemisphere and becomes the winter cell. Instead the winter cell in the Northern Hemisphere is a continuation of the summer cell in that hemisphere and hence does not need to be continuous with the winter cell in the Southern Hemisphere. The growth of the Northern Hemisphere circulation, from its summer strength of almost zero to its winter maximum strength of 7 (times the symmetric steady value), is a continuous

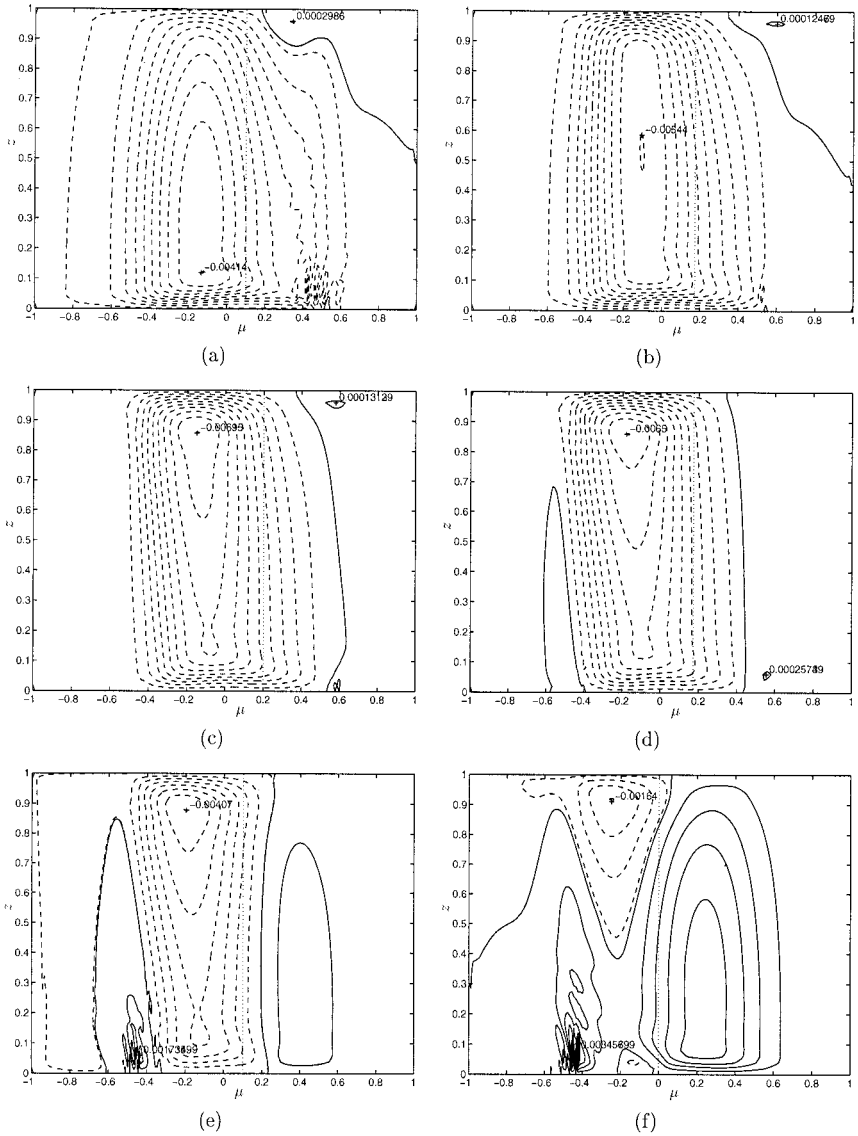

FIG. 6. Time-dependent streamfunctions for (a) one, (b) two, (c) three, (d) four, (e) five, and (f) six months; after the spring equinox.

process. At the instant when $\mu_0(t)$ crosses the equator from the Northern Hemisphere to the Southern Hemisphere, the northern circulation reaches a value of 2.5 (times the symmetric steady value). This is as depicted in Fig. 1, if μ_0 is changed to $-\mu_0$ and the strength is defined as the maximum clockwise streamfunction in the Northern Hemisphere in that figure.

In Fig. 5b we plot the latitudinal location of the maximum value of the clockwise circulation (dash–dotted line with "×") and the counterclockwise circulation (dashed line with "○"), as a function of $\mu_0(t)$ (in solid line). As $\mu_0(t)$ moves northward, the dominant circulation is the counterclockwise one with the maximum located near 10°S. As $\mu_0(t)$ returns to the equator and then moves into the Southern Hemisphere the clockwise circualtion becomes the dominant one 17 days after $\mu_0(t)$ crosses the equator. Its maximum is located near 10°N. Prior to this, the maximum values of both the clockwise and counterclockwise cells are located in the Southern Hemisphere. The former is a thermally indirect cell, called the Ferrel cell here. It is located more poleward, and has a larger strength, than the direct cell in the same hemisphere during equinoxes. Ferrel cells play a role in accelerating the switch from counterclockwise to clockwise circulation in this half of the annual cycle. This is shown next in the meridional-height plane.

The contours of the streamfunction for each month after (northern) spring equinox are shown in Fig. 6. The dashed lines show the winter cell (counterclockwise with negative values), the solid lines show the summer

cell (clockwise with positive values) and the dotted line shows the location of the heating center μ_0.

When μ_0 moves from the equator to the maximum location in the Northern Hemisphere, the strength of the winter cell in the Southern Hemisphere increases and reaches its maximum 15 days after the (southern) winter solstice. The summer cell in the Northern Hemisphere is negligible.

After the winter cell reaches its maximum, the strength of the winter cell starts to decrease monotonically as μ_0 decreases. When $\mu_0 < 0.17$, there appears a Ferrel cell in the Southern Hemisphere. The summer cell in the Northern Hemisphere starts to be enhanced as μ_0 decreases further.

When μ_0 returns to the equator at the autumn equinox, remnants of the winter—counterclockwise—cell are lifted to the upper levels. There are now two strong clockwise cells: a summer cell in the Northern Hemisphere and a Ferrel cell in the Southern Hemisphere. The indirect cell—the Ferrel cell—is stronger than the direct cell in the same hemisphere. As $\mu_0(t)$ moves into the Southern Hemisphere, the northern clockwise cell strengtherns as the Ferrel cell, which has the same sign, merges with the winter cell. This accelerates the switching to a single clockwise winter cell.

In conclusion, there are four stages in an annual cycle for the meridional circulation: 1) three months with a dominant winter cell in the Southern Hemisphere (from day 30 to day 120); 2) three months with a three-cell structure (one winter cell, one summer cell, and one Ferrel cell in the south), when the Ferrel cell is dominant in first 2 months (from day 120 to day 180) and the summer cell is dominant in the last month (from day 180 to day 210) among the clockwise cells; 3) three months with a dominant winter cell in the Northern Hemisphere (day 210 to day 300); and 4) another 3 months with a three-cell structure with a counterclockwise Ferrel cell in the Northern Hemisphere. The three-cell patterns was also suggested by Asnani (1995), with one equatorial cell separating two Hadley cells.

The time-dependent solution loses its symmetry about the equator. The circulation is never equatorially symmetric although its annual mean is. Although the time-dependent meridional circulation is quite different from its counterpart in the steady state, the annual averages of these two have almost the same in strength as well as in extent (the former is 10% weaker than the latter), provided the annual average of the steady-state solutions is taken according to (14).

b. Temperature

The behavior of the temperature distribution is easy to understand. For a steady solution, the temperature in the circulation region in our present nonlinear limit [the nearly inviscid limit of Held and Hou (1980)] is *horizontally homogenized.* This result was noted previously in numerical calculations in dry (Held and Hou 1980; Lindzen and Hou 1988) as well as moist (Satoh 1994) model atmospheres. Fang and Tung (1996) recently gave a general derivation. It is a consequence of angular-momentum conservation in the circulation core, which yields a zonal velocity that is independent of height. By thermal wind the temperature gradient then vanishes. This result depends on the steady-state assumption but is nevertheless still valid in the portion of the Tropics where there is always a persistent circulation; it does not matter that the sign of the circulation reverses from winter to spring.

Away from the circulation region, the temperature Θ approaches its radiative equilibrium value Θ_E in the steady solution. This is not the case in the time-dependent solution. It is noted that even without a meridional circulation, the temperature does not approach Θ_E. It should approach a ''dynamical equilibrium'' state Θ_D, which is determined by a local time-dependent radiative process:

$$\frac{\partial \Theta_D}{\partial t} = \frac{\Theta_E - \Theta_D}{\tau}. \tag{15}$$

With $\Theta_E(\mu, z, t)$ given by (7) and (8), we know that Θ_E consists of two harmonic components:

$$\Theta_E(\mu, z, t) = \Theta_{E0}(\mu, z) + 2\mu\mu_{0\,\max} \sin(\omega t) + 0.5\mu_{0\,\max}^2 \cos(2\omega t), \tag{16}$$

where $\Theta_{E0}(\mu, z) = \Theta_{00} - \Delta_V z - \mu^2 - 0.5\mu_{0\,\max}^2$. In high latitudes, the first harmonic component (the annual cycle) is dominant while in the equatorial region, the second harmonic component (the semiannual cycle) is dominant. Solving (14), we obtain a periodic solution as $t \to \infty$:

$$\Theta_D(\mu, z, t) = \Theta_{E0}(\mu, z) + \frac{2\mu\mu_{0\,\max}}{[1 + (\omega\tau)^2]^{1/2}} \sin(\omega t - \varphi_1) + \frac{\mu_{0\,\max}^2}{2[1 + (2\omega\tau)^2]^{1/2}} \cos(2\omega t - \varphi_2), \tag{17}$$

where

$$\varphi_1 = \sin^{-1}\frac{\omega\tau}{(1 + \omega^2\tau^2)^{1/2}};$$

$$\varphi_2 = \sin^{-1}\frac{2\omega\tau}{(1 + 4\omega^2\tau^2)^{1/2}}. \tag{18}$$

It is found that for a fast relaxation process ($\omega\tau \ll 1$), the dynamical equilibrium temperature approaches $\Theta_E(\mu, z, t)$, which is the square of sinusoidal function of latitudes with a time-dependent maximum position. For a slow relaxation process ($\omega\tau \gg 1$) Θ_D approaches a steady distribution $\Theta_{E0}(\mu, z)$, which is also the square of sinusoidal function of latitudes but with a steady maximum position at the equator. Generally speaking, Θ_D differs from Θ_E in both magnitude and phase. In high latitudes, Θ_D is primarily given by the annual har-

monic and its phase shift is φ_1; that is, Θ_D has approximately a time lag of Δt relative to Θ_E, where

$$\Delta t = \frac{1}{\omega} \sin^{-1} \frac{\omega\tau}{(1 + \omega^2\tau^2)^{1/2}}.$$

For a small $\omega\tau$, we have $\Delta t \approx \tau$. In our study, the annually varying forcing has $\omega = 2\pi\ (360\ \text{day})^{-1}$ and $\tau = 20$ days, which leads to approximately a 19-day time lag. In the equatorial region, Θ_D is primarily given by the semiannual harmonic and it has a time lag of approximately

$$\Delta t = \frac{1}{2\omega} \sin^{-1} \frac{2\omega\tau}{(1 + 4\omega^2\tau^2)^{1/2}},$$

which is about 17.5 days in our calculation.

It is clear that in the time-dependent case, Θ_D replaces the role of Θ_E as an ''equilibrium temperature.''

The distributions of the temperature and Θ_E at (northern) summer solstice and at the spring equinox are shown in Fig. 7. The distributions at the winter solstice and at the autumn equinox are reflections of these about the equator. As in the steady solution, the temperature in the Tropics is flat. In the high latitudes, in contrast to the steady solution, the time-dependent temperature has a significant deviation from its radiative equilibrium state even in the absence of the meridional circulation. It is approximately given by the dynamical equilibrium state $\Theta_D(\mu, z, t)$. The heating could be positive or negative depending on the location and the time. Unlike the case of the steady-state solution, it is now unnecessary that diabatic heating be balanced by adiabatic heating.

The time-dependent solution of the temperature, the steady solution of the temperature, the dynamical equilibrium, and the equilibrium temperature at the level of $z = 0.5$ and at various latitudes are shown in Fig. 8 as functions of the heating center μ_0. The dashed line is for Θ_E, the dash–dotted loop for Θ_D, the solid loop for the calculated temperature, and the steady solution are shown in scattered points marked by *. The detail of the numerical result for the periodic solution is described in the following.

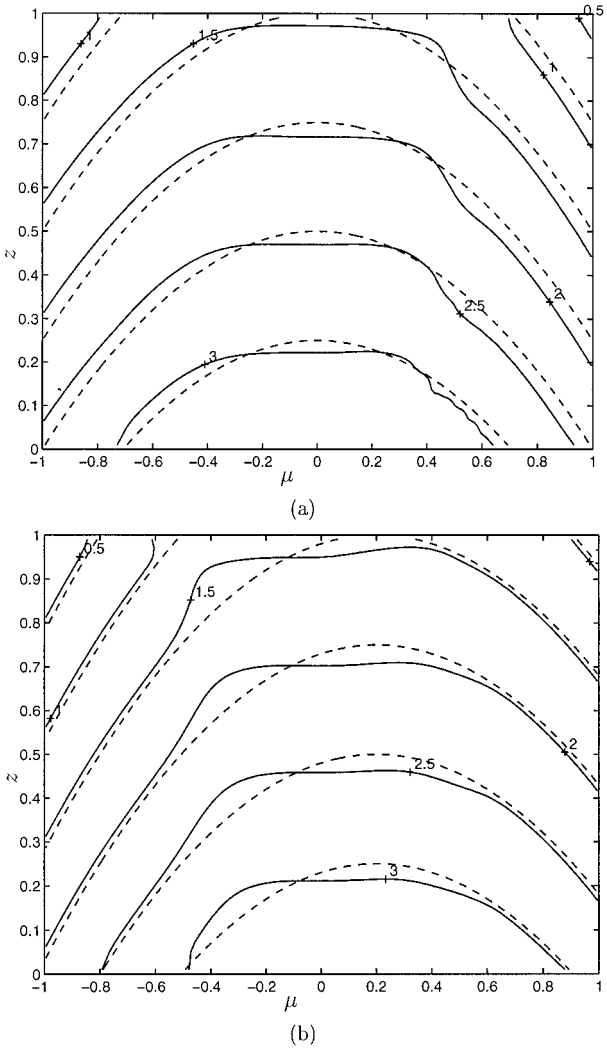

FIG. 7. Temperature (solid lines) and equilibrium temperature (dashed lines) distributions at (a) the spring equinox and (b) the summer solstice. The solutions at the autumn equinox and the winter solstice are reflections of these about the equator. The temperature contours shown are $(T - 125\ \text{K})/50\ \text{K}$.

1) It can be seen that the temperature at the equator (see Fig. 8a) has the same time pattern as Θ_D (which is dominated by the semiannual component) but is colder. Both reach their maximum about 18 days after the equinoxes. In the Tropics ($-0.3 \le u \le 0.3$), the temperature Θ has almost the same pattern as that at the equator (compare Figs. 8b and 8a) despite the fact that Θ_D and Θ_E vary significantly. This is due to the temperature homogenization effect by the meridional circulation discussed in Fang and Tung (1996).
2) In the subtropics ($\mu = 0.4$–0.5; see Fig. 7c), which are near the edge of the circulation, the effect of the meridional transport on the temperature exists in part of the annual cycle only. The temperature is controlled by the equatorial temperature in this part of the annual cycle and is controlled by the high-latitude temperature (Θ_D) at other times. The temperature increases monotonically as μ_0 increases but with a time lag of approximately 30–45 days.
3) In mid- to high latitudes ($\mu = 0.6$–0.8; see Fig. 8d), Θ is close to its dynamical equilibrium Θ_D. Here Θ_E is in the same phase as $\mu_0(t)$ while Θ_D and Θ have a time lag. These are all dominated by the annual component. The temperature attains its maximum and its minimum when it equals its dynamical equilibrium value.
4) Compared to the steady solution, the time-dependent temperature is less sensitive to the displacement of the heating center off the equator. There is no abrupt

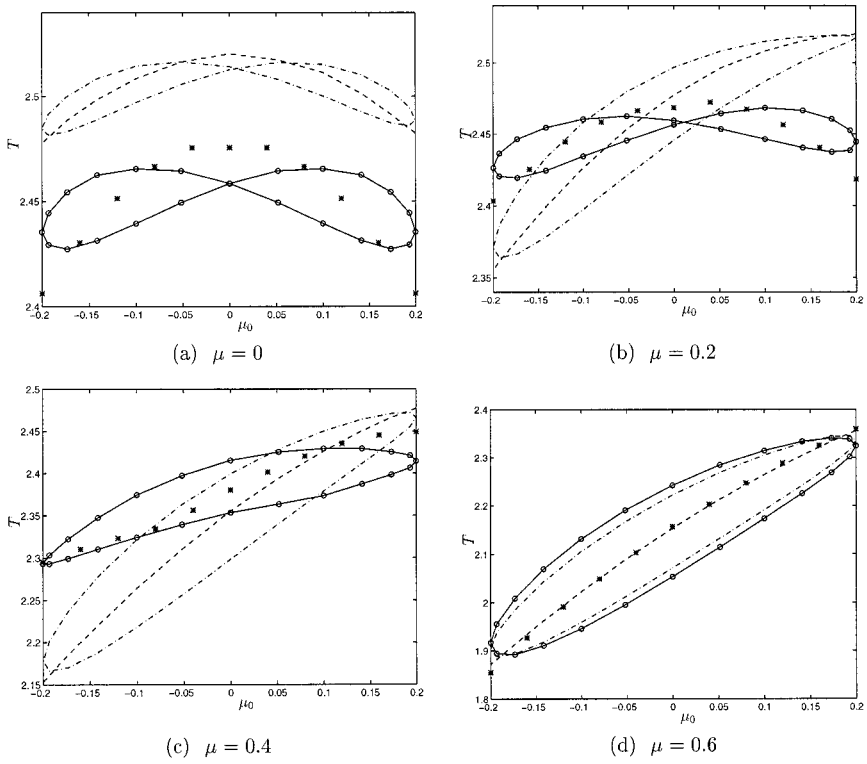

FIG. 8. Time-dependent solution of temperature (solid line with "○"), dynamical equilibrium temperature (dash–dotted line), equilibrium temperature (dashed line), and the steady solution of temperature (marked by *) at $z = 0.5$ for (a) $\mu = 0$, (b) $\mu = 0.2$, (c) $\mu = 0.4$, and (d) $\mu = 0.6$. The temperature is scaled as in Figs. 2 and 7.

change as the heating center crosses the equator in its annual march.

5) In general, the temperature and the zonal wind are still related by the geostrophic balance in both the circulation region and the high latitudes. The temperature in the high latitudes can be obtained by the linearized thermodynamic equation, while in the Tropics it is given by the temperature at the equator with a flat meridional gradient; that is, the temperature is homogenized in the Tropics. This situation is the same as in the steady solution, although the homogenized region is narrower than that in the steady solution. This homogenization is due to a persistent meridional circulation in the Tropics. The region where there is a persistent meridional circulation during most of the year is narrower than in the steady solution. The annual average of the time-dependent temperature is, however, almost identical to that for the steady solution in this region.

As in the steady-state solution, the zonal wind and the temperature satisfy in the time-dependent solution the geostrophic balance in the parameter region that we are in. It is close to its dynamical equilibrium state in high latitudes (with temperature given by the dynamical equilibrium temperature Θ_D) and is close to an absolute-angular-momentum-conserving solution in the Tropics, while the zero wind line is usually not at the heating center.

5. Concluding remarks

In this paper, we have reviewed the steady solution corresponding to various displacements of the heating center and compared it with the time-dependent solution corresponding to an annually varying heating. Since the solution of the model is strongly nonlinear, it is to be expected that the average of the solutions for different heatings is not necessarily the same as the solution corresponding to the averaged heating. Thus, although the annually averaged heating is symmetrically centered at the equator, the annually averaged circulation forced by an annually varying heating is stronger, by a factor of 2, than the circulation forced by the annually averaged heating. This is even more remarkable when it is noted that the annual average includes 3 months during the summer when the local circulation is almost nonexistent.

Our systematic study confirmed that the steady solution is qualitatively in good agreement with the time-dependent solution in the following respects. (i) The meridional plane is divided into a circulation region in the Tropics and a no-circulation region at high latitudes; (ii) in the circulation region, the horizontal temperature

gradient is weak and the zonal wind approximately satisfies the absolute-angular-momentum conservation; (iii) the geostrophic balance is still satisfied approximately; and (iv) the circulation in the winter hemisphere is stronger than that in the summer hemisphere except near the equinoxes.

Although there is almost no difference between their ''temporal'' averages, if for the steady state the annual average is properly defined, the time-dependent solution does have some features that are different from the steady solution.

1) There is no abrupt change of the strength of the Hadley circulation as the heating center is moved off the equator in its annual march. In the steady-state solutions, there is a sensitive dependence on the displacement of this location off the equator.
2) As the heating center moves poleward, the positions of the zonal jets move equatorward slightly, which is different from the result obtained in the steady solutions.
3) In the time-dependent study, the dynamical equilibrium temperature plays the role of the ''radiative equilibrium'' temperature. It is obtained from a circulation-free, radiatively controlled equation. This temperature has a phase shift from the change of the heating center, which depends on the relaxation time τ, the annual frequency ω, and the form of the thermal equilibrium temperature.
4) The Ferrel cells are an obvious feature of the time-dependent solution during the equinoxes, while they are almost negligible in the steady solution.

It should be noted that the Newtonian cooling parameterization used in this study may not be appropriate to the real atmosphere, where moist convection tends to occur in a narrow latitudinal band. Numerical calculations for a model with a narrow heating region such as in an ITCZ were also performed. When compared to the steady-state solution of Fang and Tung (1996), which showed an abrupt increase in circulation strength as the ITCZ is displaced off the equator, the time-dependent solution shows a continuous transition, similar to that discussed in this paper.

It is noted that the external thermal condition in the real atmosphere is not equatorially symmetric in an annual cycle due to the different land–sea contrasts in two hemispheres. Therefore, the periodic equilibrium temperature that we used in this paper is an idealization only.

Acknowledgments. We wish to thank Dr. Hu Yang and Professor Christopher Bretherton for their valuable discussions. This research is supported by NSF Grant ATM 9526136 and NASA Grants NAG-l-1404 and NAG 5-2802.

REFERENCES

Asnani, G. C., 1995: Comments on ''Dynamics and energy balance of the Hadley circulation and the tropical precipitation zones: Significance of the distribution of evaporation.'' *J. Atmos. Sci.,* **52,** 614–618.

Fang, M., and K. K. Tung, 1994: Solution to the Charney problem of viscous symmetric circulation. *J. Atmos. Sci.,* **51,** 1261–1272.

——, and ——, 1996: A simple model of nonlinear Hadley circulation with an ITCZ: Analytic and numerical solutions. *J. Atmos. Sci.,* **53,** 1241–1261.

——, and ——, 1997: The dependence of the Hadley circulation on the thermal relaxation time. *J. Atmos. Sci.,* **54,** 1397–1384.

Hack, J. J., and W. H. Schubert, 1990: Some dynamic properties of idealized thermally-forced meridional circulations in the Tropics. *Meteor. Atmos. Phys.,* **44,** 101–117.

——, ——, D. E. Stevens, and H. Kuo, 1989: Response of the Hadley circulation to convective forcing in the ITCZ. *J. Atmos. Sci.,* **46,** 2957–2973.

Held, I. M., and A. Y. Hou, 1980: Nonlinear axially symmetric circulations in a nearly inviscid atmosphere. *J. Atmos. Sci.,* **37,** 515–533.

Hou, A. Y., and R. S. Lindzen, 1992: The influence of concentrated heating on the Hadley circulation. *J. Atmos. Sci.,* **49,** 1233–1241.

Lindzen, R. S., 1990: *Dynamics in Atmospheric Physics.* Cambridge Press, 310 pp.

——, and A. Y. Hou, 1988: Hadley circulation for zonally averaged heating centered off the equator. *J. Atmos. Sci.,* **45,** 2416–2427.

Liu, Z. R., and M. Mak, 1995: Impacts of SST on the Hadley circulation. Preprints, *10th Conf. on Waves and Stability,* Big Sky, MT, Amer. Meteor. Soc., 95–96.

Plumb, R. A., and A. Y. Hou, 1992: The response of a zonally symmetric atmosphere to subtropical thermal forcing: Threshold behavior. *J. Atmos. Sci.,* **49,** 1790–1799.

Satoh, M., 1994: Hadley circulation in radiative-convective equilibrium in an axially symmetric atmosphere. *J. Atmos. Sci.,* **51,** 1947–1968.

Schneider, E. K., 1977: Axially symmetric steady-state models of the basic state for instability and climate studies. Part II. Nonlinear calculations. *J. Atmos. Sci.,* **34,** 280–296.

——, and R. S. Lindzen, 1977: Axially symmetric steady-state models of the basic state for instability and climate studies. Part I. Linearized calculations. *J. Atmos. Sci.,* **34,** 263–279.